Analytical Simulation of Nonlinear Response to Seismic Test Excitations of HDR-VKL Piping System

M. G. Srinivasan, C. A. Kot
Argonne National Laboratory, Argonne, IL 60439, USA
and
Masoud Mojtahed
Mechanical Engineering
Purdue University Calumet, Hammond, IN 46323, USA

ANL/CP--71269

DE91 015989

1 INTRODUCTION

Dynamic tests with simulated earthquake excitation (SHAM) were performed during April–May 1988 on the Versuchskreislauf (VKL) piping system at the Heissdampfreaktor (HDR) Test Facility in Kahl/Main, Federal Republic of Germany. The major objectives of these tests were to study the behavior of a full-scale in-plant piping system subjected to a range of seismic excitation levels (from design levels to those that might induce either failure of pipe supports or plasticity in the pipe runs) and to establish seismic margins for piping and pipe supports. Data obtained in the tests are also being used to validate analytical methods for piping response calculation. Detailed reports on the SHAM experiments are given elsewhere by Kot et al. (1990).

This paper describes an effort to evaluate the computer code NONPIPE (proprietary to Nutech Engineers) with data from one of the SHAM tests. NONPIPE is a nonlinear finite-element program capable of calculating the elastic-plastic response of piping systems subjected to seismic excitation. The special characteristic of this code is the simplified or approximate approach it uses for modeling the elastic plastic behavior which makes the calculations relatively less resource intensive than those of other nonlinear codes. The evaluation is based on a comparison of computational results of simulation of a SHAM test with corresponding test measurements.

2 DESCRIPTION OF TESTS

Figure 1 shows the VKL piping system. The pipe runs of the VKL, excluding the HDU vessel, extend about 10 m in the vertical direction, about 11.5 m in the x direction, and about 6 m in the z direction. The pipes are of stainless steel, ranging from 100 to 300 mm in diameter. The HDU vessel was fixed at its base, and a displacement restraint in the x and z directions was provided by a structural frame located about one-third of the height of the vessel from its top. The DF15 manifold was directly attached to the floor, as indicated schematically in Fig. 1. Six different seismic support configurations, designed by different participants in the SHAM experiments (Kot et al., 1990), were used during the dynamic tests. Figure 1 shows a configuration with struts only for seismic supports. This is designated as the KWU configuration for identification purpose only.

During the SHAM tests, the dynamic excitation along the x direction was applied to two different points of the piping with the H5 and H25 actuators, as shown in Fig. 1. The excitation time-histories represented an integral multiple of a hypothetical safe-shutdown earthquake (SSE) with a peak acceleration of 0.6 g. The tests covered a range of excitation levels from 100 to 800% SSE. This paper concerns a test of the highest level of excitation, viz., 800% SSE, of the KWU configuration.

3 ANALYTICAL SIMULATIONS

Both pretest predictions and posttest simulations of the linear response of the VKL system for different support configurations for low-level excitations have been performed in the past. Earlier reports

DISCLAIMER

(Kot et al., 1990, Srinivasan et al., 1989, Srinivasan et al., 1990) gave the results of the pretest and posttest linear simulations. The finite element model devised for the linear simulations was used, with some changes, for the nonlinear simulation with the NONPIPE code. The major changes to the model for the NONPIPE calculations were the introduction of material properties in the plastic regime and the replacement of single curved pipe elements for elbows with multiple straight pipe elements.

3.1 Description of NONPIPE approach

The NONPIPE code is a finite-element program capable of determining the nonlinear dynamic response of piping systems of arbitrary configuration subjected to force or acceleration time histories. The nonlinearities modeled are elastic-plastic material behavior, gaps in connection to supports, and large displacement effects arising due to substantial change in direction of restraints. For the present problem the only nonlinearity considered was the elastic-plastic behavior.

Elastic-plastic behavior is modeled by assuming the moment-curvature and torque-twist relationships to be trilinear. Strain hardening is approximated by considering the pipe element to consist of three parallel pipe elements, each with its own elastic-plastic or elastic behavior derived from the trilinear relationship (Nutech Engineers, 1984).

The Direct Stiffness method is used to perform the analysis in which the coupled equilibrium equations are solved for each step with a constant average acceleration assumption. The stiffness is modified each time a change in the yield status of the structure occurs, and correction forces are applied at the end of each time step to ensure that the dynamic equilibrium is continually satisfied.

3.2 Finite-Element Model

The entire system shown in Fig. 1 was modeled with pipe and spring elements only. Concentrated masses were added to the appropriate nodes to represent the actual mass of the parts represented by artificial elements. A similar technique was used for modeling the tees and the valves. Each pipe elbow was modeled by means of five straight elements. The model comprised 266 pipe elements. The total mass of the modeled system was about 74,800 Kg.

The pipe supports were modeled with spring elements. The constant-force hangers H16, H17, H18, and H19 were ignored since they were assumed not to respond to dynamic excitation. Although appropriate stiffness was assumed to represent each of the remaining pipe supports, no distinction was made as to the behavior of struts and spring hangers when subjected to dynamic excitation. The two sway struts of H23 were represented by a single spring element.

3.3 Inputs to Analysis

The NONPIPE code does not provide for specifying multiple independent acceleration input. However, it does allow independent force histories to be prescribed. Both the acceleration and the displacement histories applied at each of the two actuators, H5 and H25, showed that the two inputs were not the same. Therefore it was necessary to apply the excitation in the form of equivalent force histories at H5 and H25.

The equivalent force may be determined by the introduction of an artificial boundary spring element (with a stiffness that is many times larger than the largest stiffness in the system) at the excitation point. The force obtained as a product of the measured displacement and the stiffness of the introduced spring is applied to the spring element at its wall end.

Two spring elements were introduced, one each at H5 and H25. The stiffness of each of these elements was defined to be about a million times larger than that of the stiffest spring element. The excitation displacement histories were scaled up by the stiffness and defined as forces at H5 and H25.

The excitation actually begins at about 0.7 s after the clock is turned on and that the peak values for the histories occur before 5 s. Therefore, the responses were determined only for the time between 0.7 s to 5.5 s. The digitization interval for the excitation histories was 0.0048624 s. The increment between analysis time steps was a fourth of the above, i.e. 0.0012156 s. Before the final computation, a parameter study was performed to ensure that the time step chosen did not give rise to significant error.

Strain hardening properties were specified for all the pipe elements except those that modeled such components as valves. NONPIPE computes the trilinear moment-curvature and torque-twist relationship for each pipe cross section, using the section and material properties and making some approximation assumptions (Nutech Engineers, 1984).

The two parameters to describe damping, α and β, were selected such that for the frequency range of 3 to 11 Hz, the damping was in the range of 2 to 3%. For frequencies below 3 Hz the damping increased with decreasing frequency and for frequencies above 10 Hz the damping increased with increasing frequency. Because the frequency content of the excitation was mostly within the frequency range noted above, the higher damping outside this range is not of concern.

4 RESULTS OF CALCULATION COMPARED WITH MEASUREMENTS

Displacements corresponding to 16 measurement channels, forces in all the struts and variable-force hangers, and bending and shear strains at 11 measurement locations were computed. Only a few of these are presented here. Figure 2 shows the locations for which comparisons of calculated and measured responses are given.

Figures 3-5 show the comparison of displacement components at gage location QN101. At this location the *z* component is better estimated than the other two components. Much better comparison for the *x* component is obtained at location QN122 as seen in Figure 6. In general, when all the comparisons are considered, the *z* components were overestimated by 15 to 35 %. About half of the *y* components were underestimated while the other half were overestimated. Two out of the three *x* components computed were close to the measurements.

Figure 7 shows the comparison of axial forces in strut H10. The peak force is only slightly underestimated and the waveform for the force is very closely predicted. The forces in H9 and H11, not shown, are also only slightly over- and underestimated respectively. The wave forms again are closely estimated. The peak forces in H4 and H23 are underestimated by 14%, and 60% respectively. In general, the strut forces are underestimated to various degrees, with H9 being the only exception.

Figures 8 and 9 show the bending strains at two straight pipe sections, RA760 and RA763. These two locations are among the highly strained straight pipe sections at which measurements were made. At each section, a bending strain is labeled as *y* or *z* strain, corresponding to whether the strain is at the extreme fiber intersecting the local *y* or *z* axis respectively. The local *x* axis coincides with the pipe axis. At RA760, the calculated *y*-bending strain closely matches the measurement. However, the *z*-bending strain (not shown) at this location does not match well, with the calculation overestimating the strain. At location RA763 the calculated *y*-bending strain (not shown) is close to the measurement only up to about 4.2 s after which it deviates from the measurement. The calculated *z*-bending strain also deviates significantly from the measurement after about 4.2 s. This location is somewhat of an outlier in that the bending strain at no other location deviates as much from the measurement as at this. The comparison of bending strains at many cross sections shows that for most sections the wave form of the calculated bending strains does resemble that of the measurements. At locations other than the two shown, about half of the peak values are overestimated by 23 to 113% and the other half are underestimated by 10 to 33%.

Figure 10 shows the comparison of measurement and calculation for shear strains at RA760. As in the case of bending strains at RA763, the calculated shear strains also begin to significantly deviate from measurement after about 4.2 s. For times smaller than 4.2 s, the calculation and measurement show similar trends and amplitudes though the waveforms do not match closely. Almost all the straight pipe sections for which comparisons were made show the same characteristics. The peak values at all straight pipe sections are overestimated by 15 to 381% mainly because of this deviation after 4.2 s. At the sections that are near elbows or tees, the calculations underestimate the peaks at three locations by 10, 42 and 45%, and overestimate the peak at two locations by 15 and 99%.

5 DISCUSSION AND CONCLUSION

Visual comparison of all the calculated histories with their measured counterparts showed that, qualitatively, the calculation results were hard to characterize as generally overestimates or underestimates. For some locations the time trend and amplitude were close to the measurement, for others

they were different. For the most part the calculations give waveforms similar to those measured except in the case of strains for which large discrepancies occur for later times.

A possible source of error in the estimated strut forces, is the neglecting of gaps in the connections of supports to pipes. Examination of the test responses shown in Fig. 7 reveals that there were higher frequency oscillations in the measurements that are not evident in the calculations. Impacts that occurred as the gaps closed might be responsible for these higher frequency oscillations.

There are two probable reasons for the large discrepancies in some of the strain estimates. The first is the approximations involved in calculating the trilinear moment-curvature (and torque-twist) relationships although this is not expected to be very significant. The second and more significant factor concerns the large deviations for times beyond 4.2 s.

The elastic-plastic properties used for the materials and given in this analysis were obtained from test specimens that did not come from the actual pipe runs of the VKL system. They are most probably from similar pipes that have never been loaded beyond initial yield. On the other hand, the actual pipes of the VKL had undergone a loading history that included repeated loading and unloading beyond the initial yield of the pipe. As a consequence of this, much of VKL piping had strain-hardened well beyond yield before the beginning of the test under consideration here, as documented by Schrammel et al. (1988) for a location close to RA760. Consequently the analytical model was 'softer' than the actual pipe material. This seems to have caused the NONPIPE calculations to show significant ratcheting to occur at a time approximately about 4.2 s at many straight pipe sections. Since shear strains are better indicators of yielding than individual bending strains, many shear strain estimates show this as is illustrated clearly by Fig. 10.

Considering the nonlinear nature of the problem and the approximations involved in modeling inelastic behavior, the discrepancies in the NONPIPE-calculated response estimates are not unreasonably large. In the case where information on the actual inelastic behavior of materials is available, NONPIPE might be an acceptable code for calculating an approximate estimate of plastic deformations.

ACKNOWLEDGMENT

This work was performed under the sponsorship of the U.S. Nuclear Regulatory Commission, Office of Nuclear Regulatory Research. The authors wish to thank Dr. Akhil Gantayat of Nutech Engineers and author of the NONPIPE code for his expert help during the model preparation and for the timely completion of the tasks for executing NONPIPE runs.

REFERENCES

Johnson, J. J., Goudreau, G. L., Bumpus, S. E., and Maslenikov, O. R. (1981). "Phase I Final Report— SMACS—Seismic Methodology Analysis Chain with Statistics (Project VIII)," NUREG/CR-2015, Vol. 9., Lawrence Livermore Laboratory.

Kot, C. A., Srinivasan, M. G., Hsieh, B. J., Malcher, L., Schrammel, D., Steinhilber, H., and Costello, J. F. (1990). "SHAM: High-Level Seismic Tests of Piping at the HDR," *Nuclear Engineering and Design*, V. 118, pp 305-318.

Nutech Engineers. (1984). Program NONPIPE Version 5.3 - User's Manual, NUTECH Engineers, San Jose, California.

Schrammel, D., Steinhilber, H., and Malcher, L. (1988). "Servohydraulische Anregung Maschinentechnik - Quick Look Report Versuchsgruppe SHAM Versuch T41" (in German), PHDR Technical Report No. 86-88, Kernforschungszentrum Karlsruhe, page 29.

Srinivasan, M. G., Kot, C. A., and Hsieh, B. J. (1989). "Response of HDR-VKL Piping System to Seismic Test Excitations - Comparison of Analytical Predictions and Test Measurements," *Trans. Tenth International Conference on Structural Mechanics in Reactor Technology*, Vol. K2, pp. 751-756.

Srinivasan, M. G., Kot, C. A., and Hsieh, B. J. (1990). "Analytical Simulation of Seismic Testing of VKL Piping System at the HDR Test Facility," *Seismic Engineering - 1990, The 1990 Pressure Vessels and Piping Conference, Nashville, Tennessee*, PVP-Vol. 197, ASME, New York, NY, pp. 175-182.

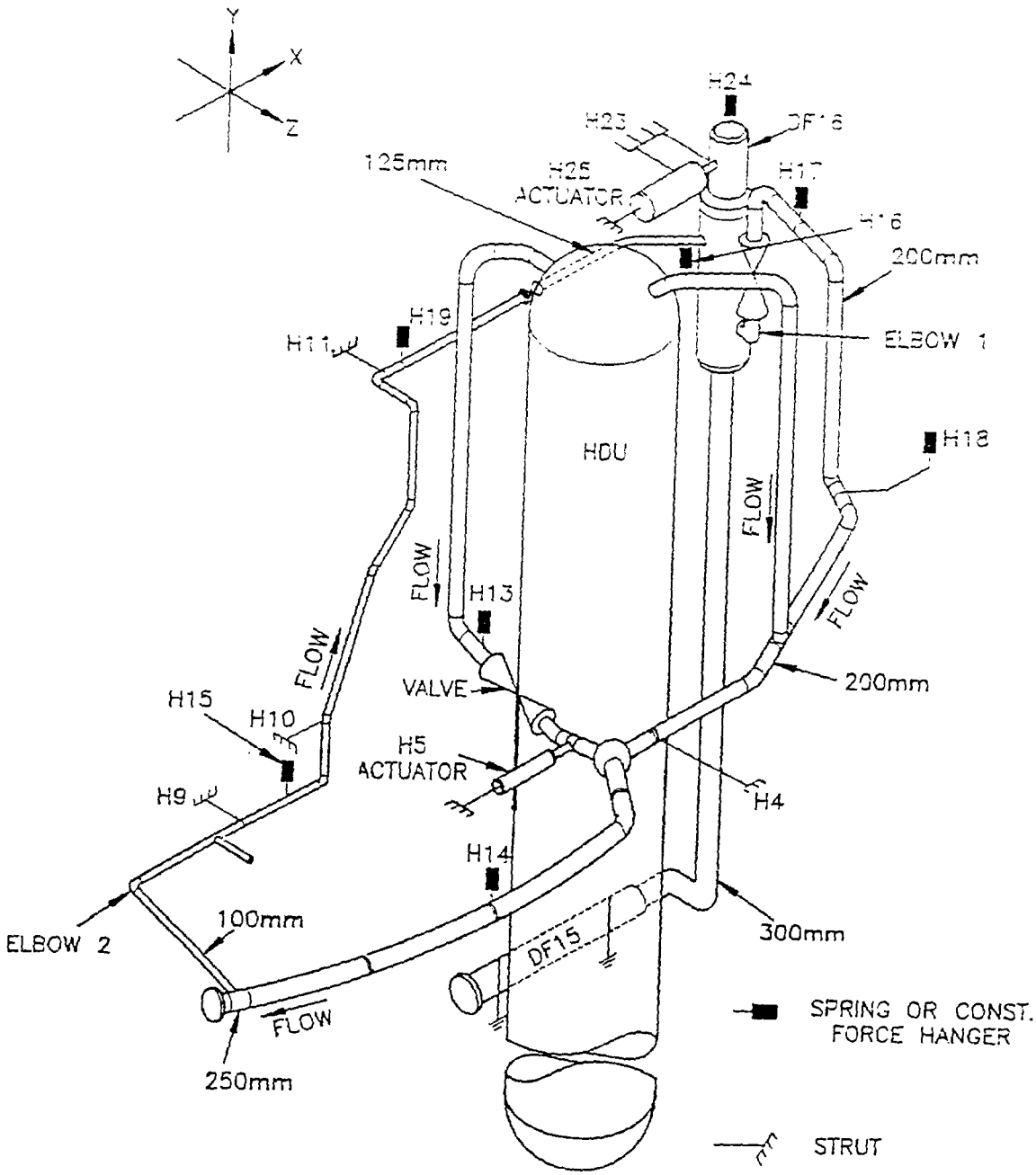

Figure 1. VKL Piping System with KWU Support Configuration

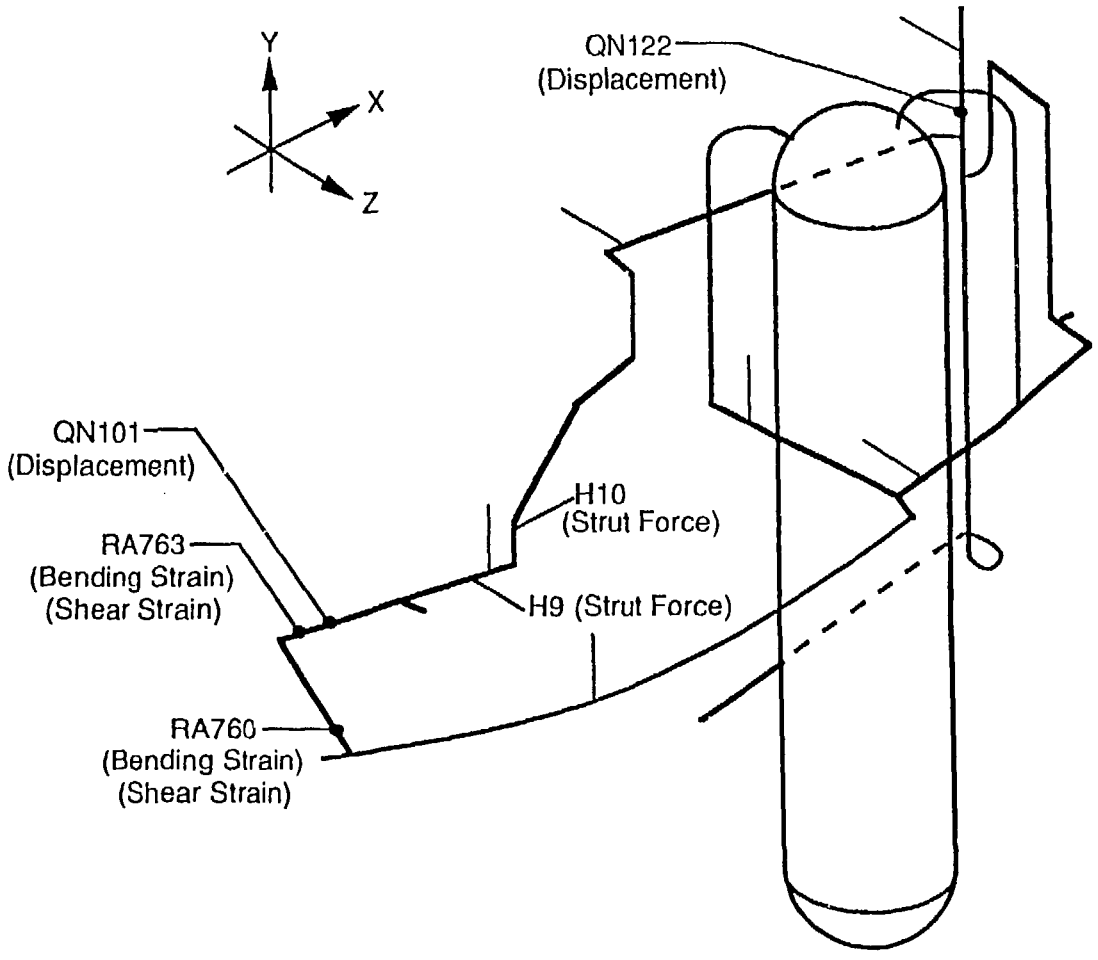

Figure 2 Locations for comparisons of response

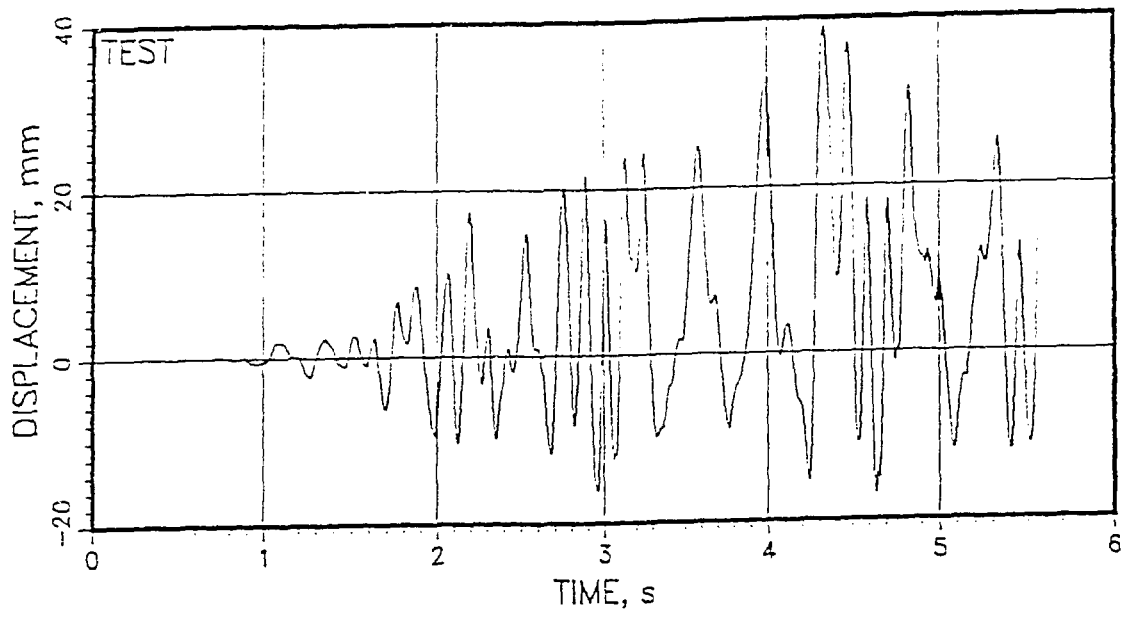

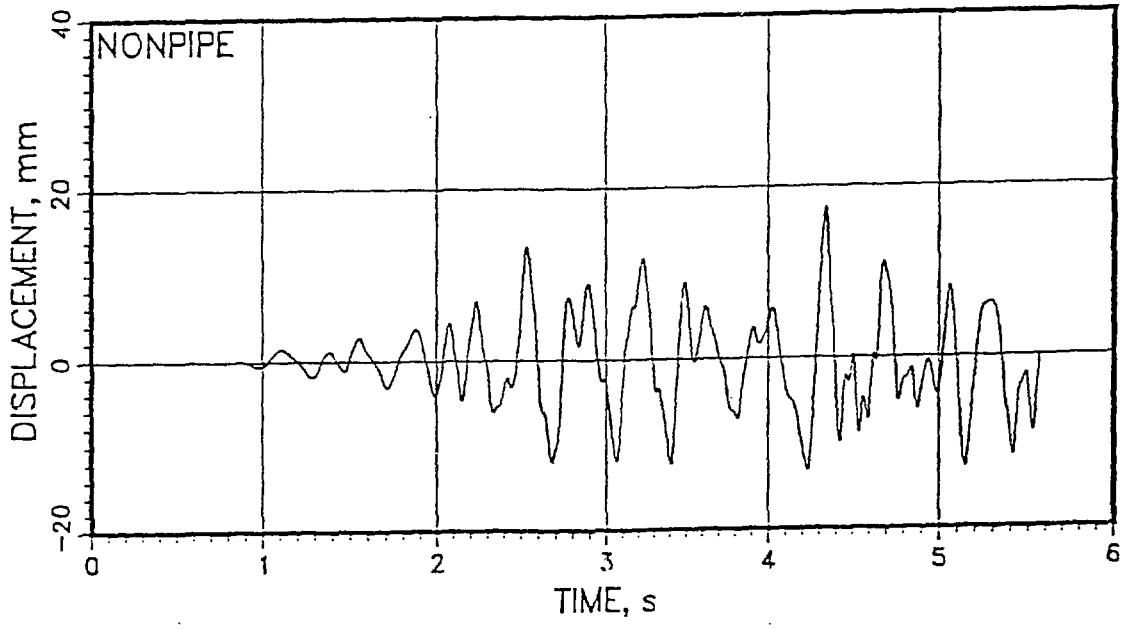

Figure 3 Comparison of measured and calculated x displacement at QN101

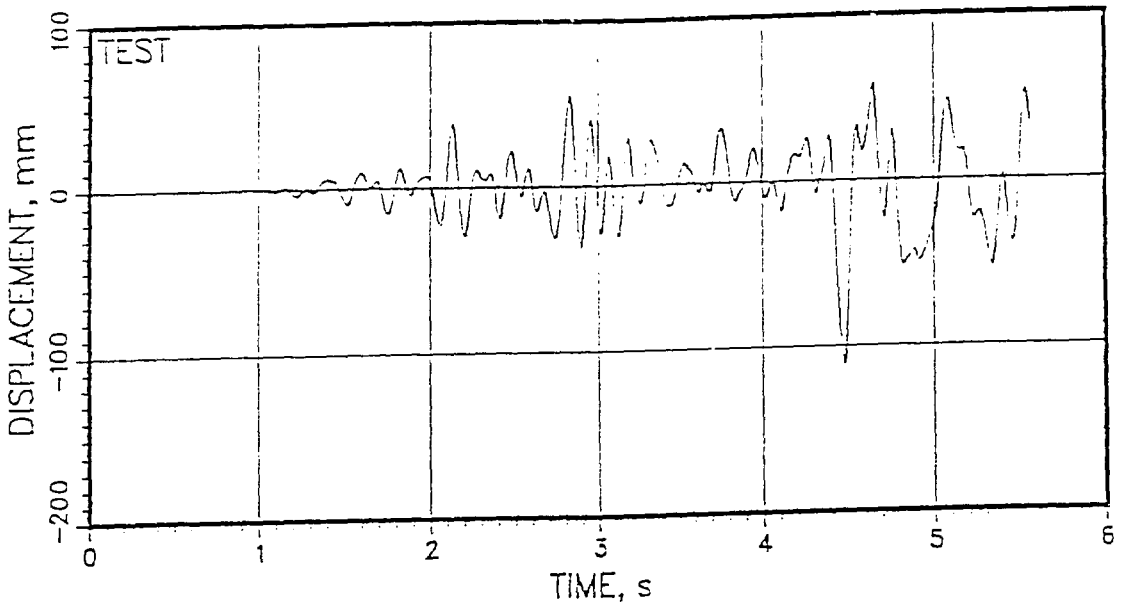

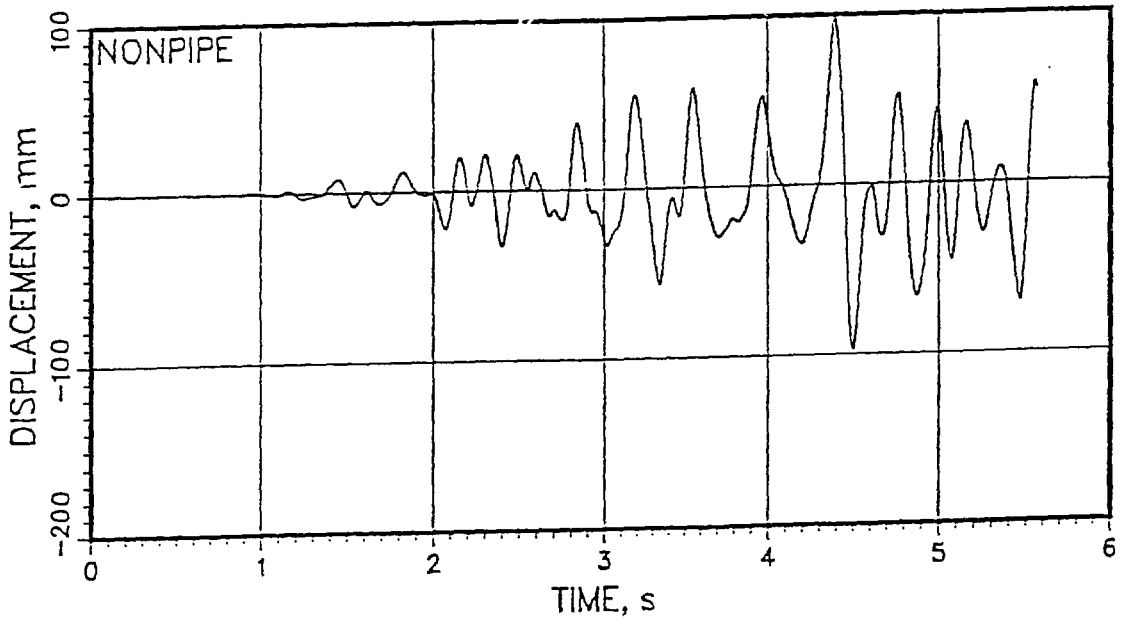

Figure 4 Comparison of measured and calculated y displacement at QN101

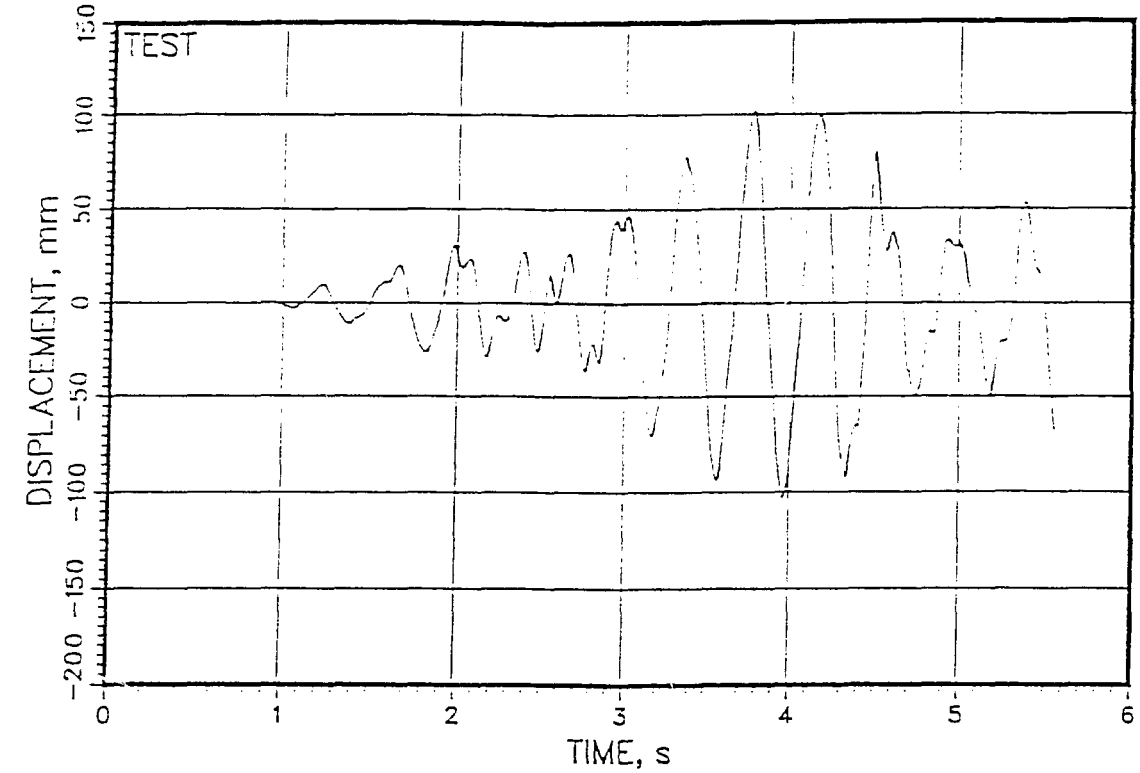

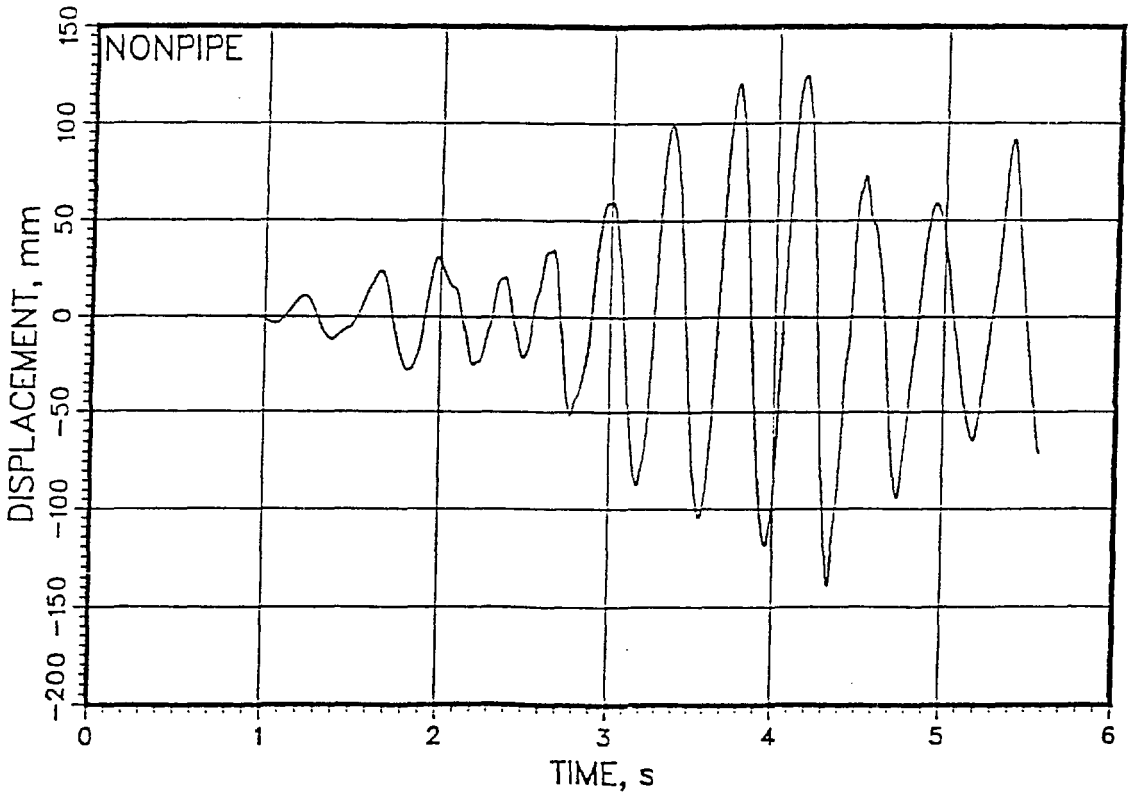

Figure 5 Comparison of measured and calculated z displacement at QN101

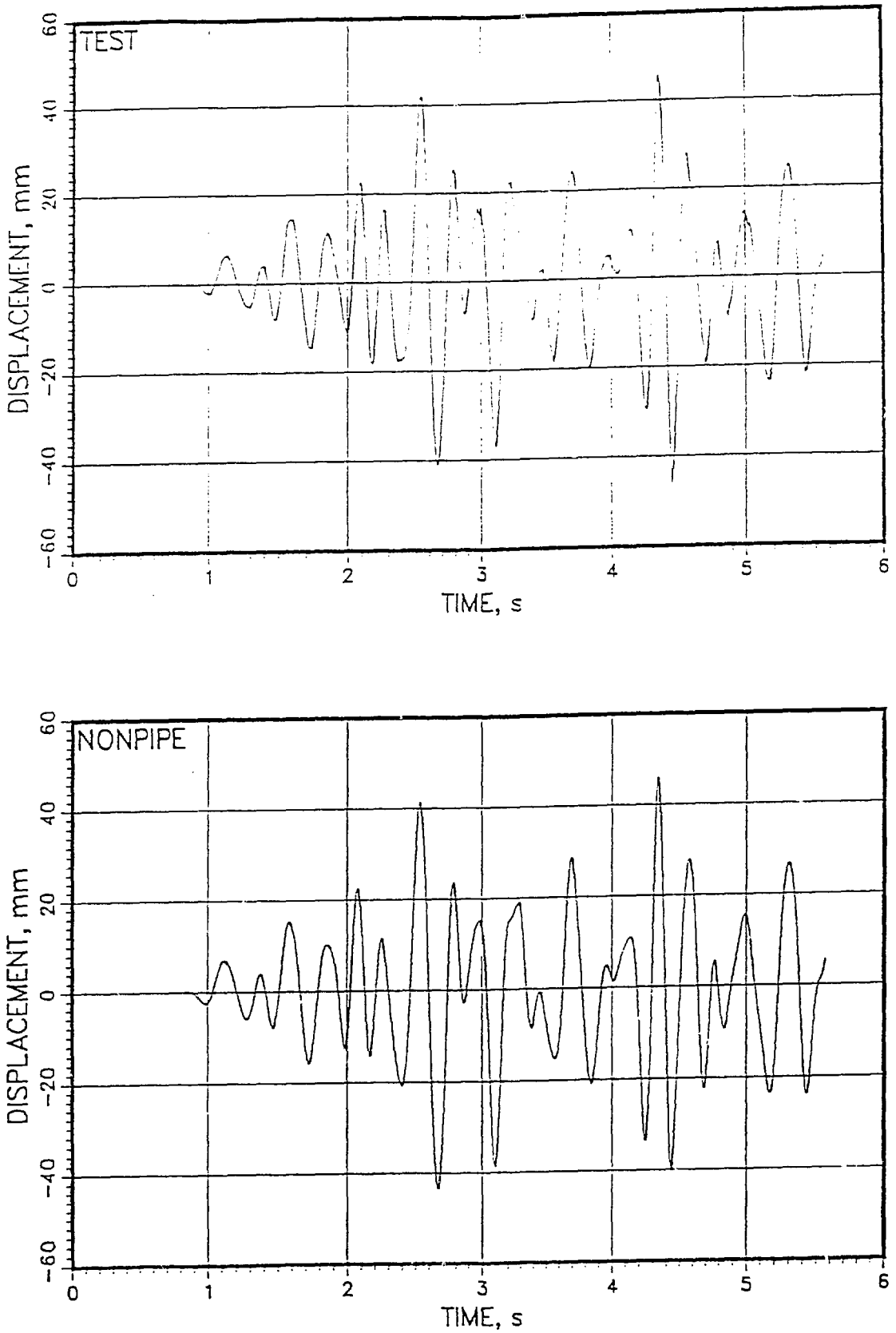

Figure 6 Comparison of measured and calculated x displacement at QN122

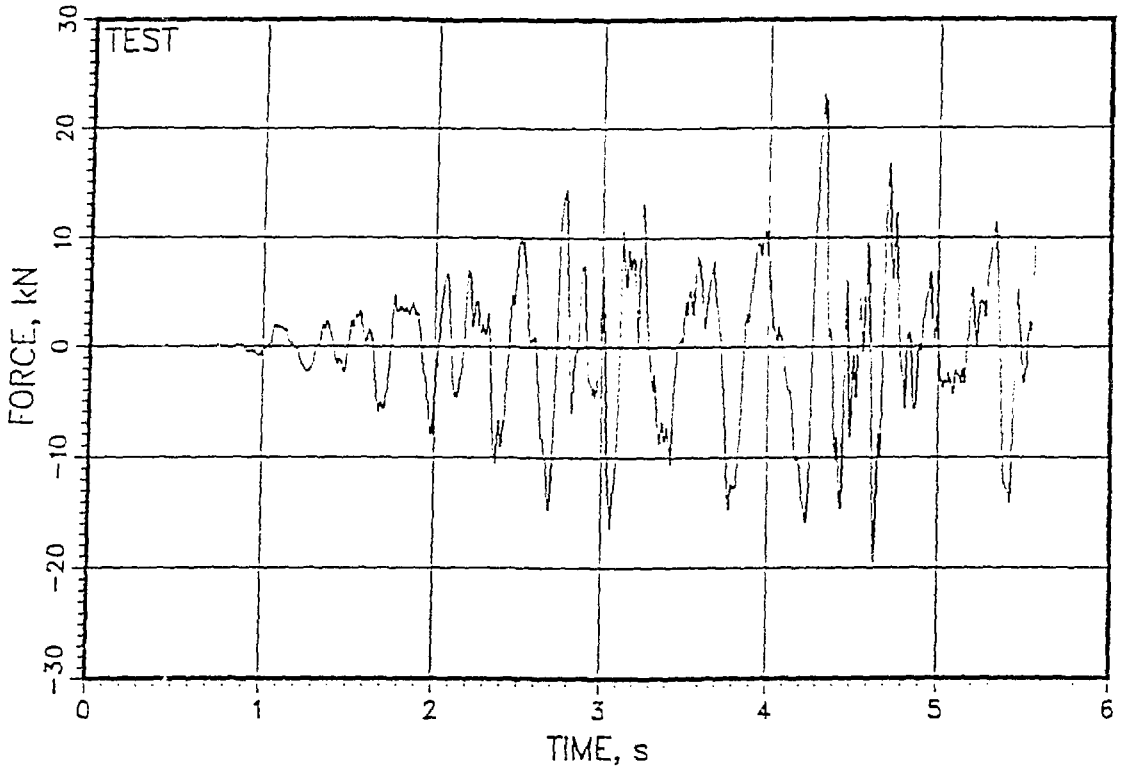

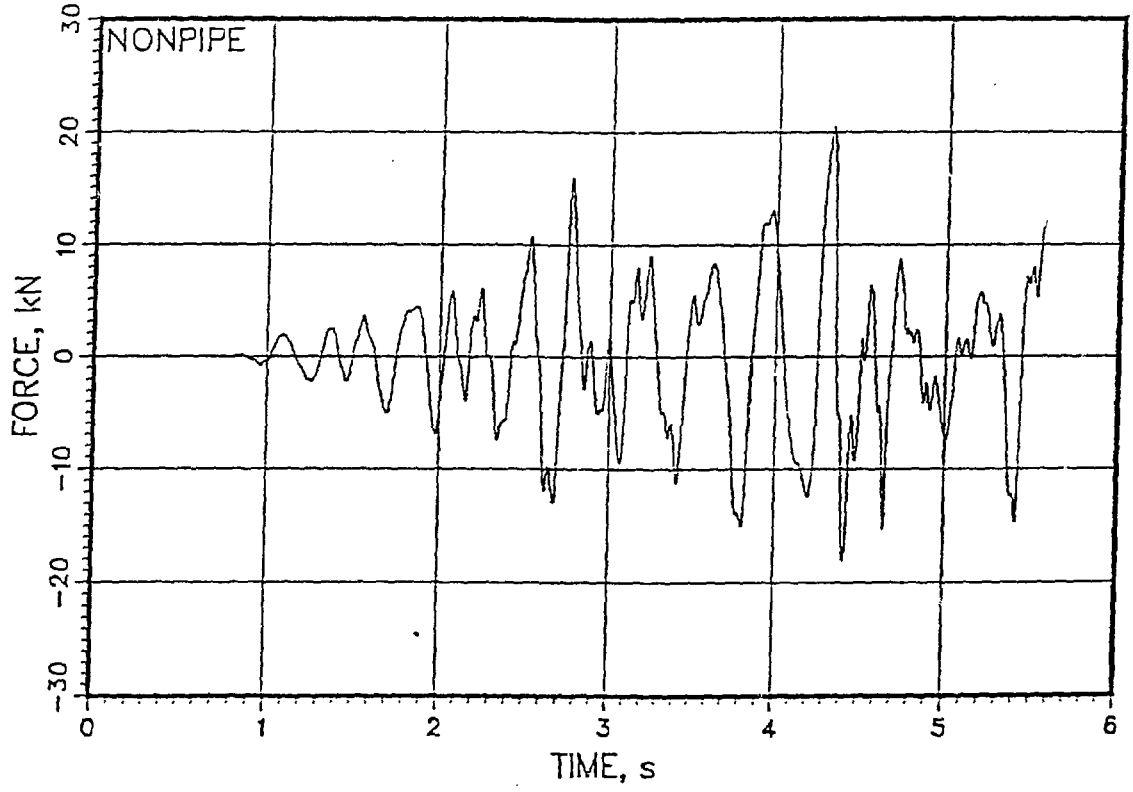

Figure 7 Comparison of measured and calculated force in strut H10

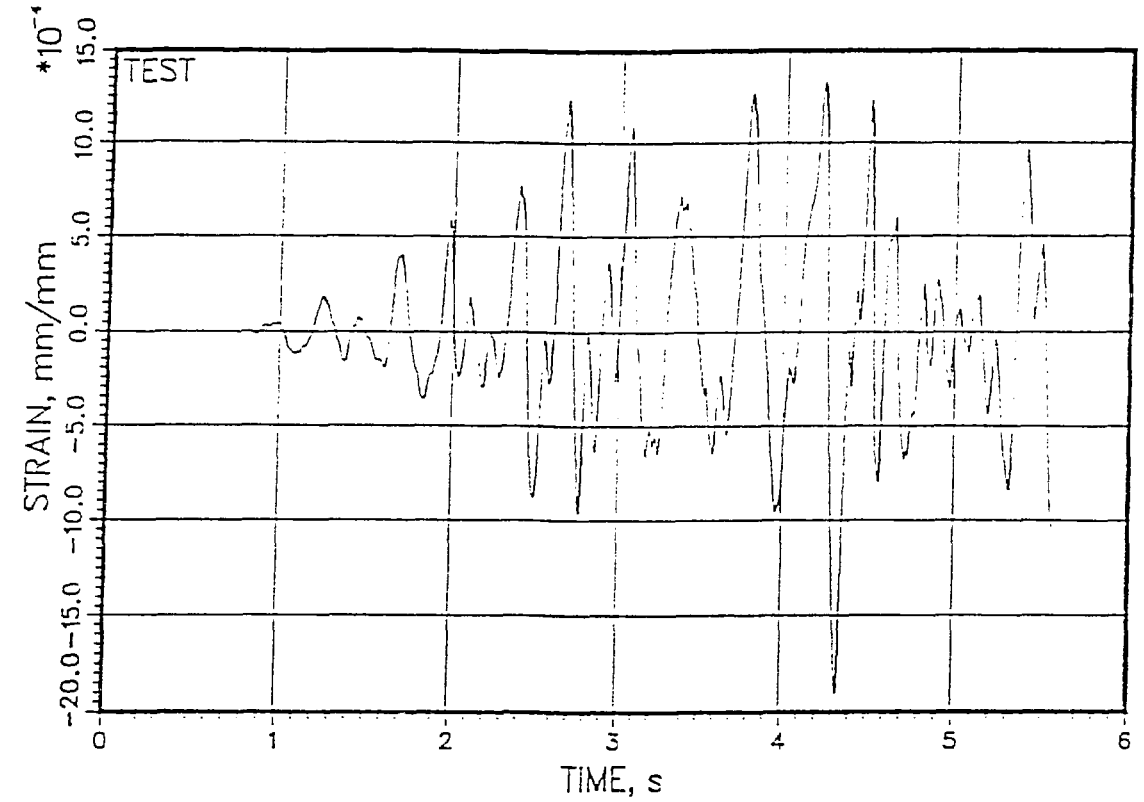

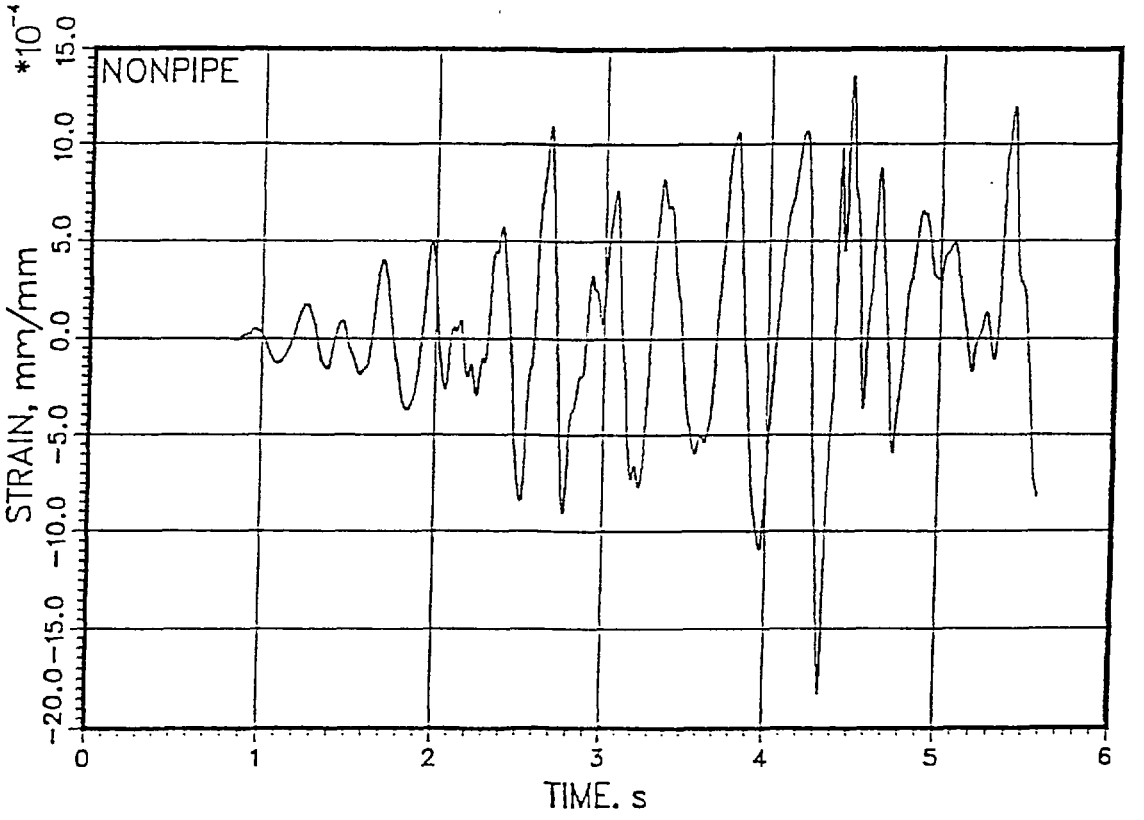

Figure 8 Comparison of measured and calculated y-bending strain at RA760

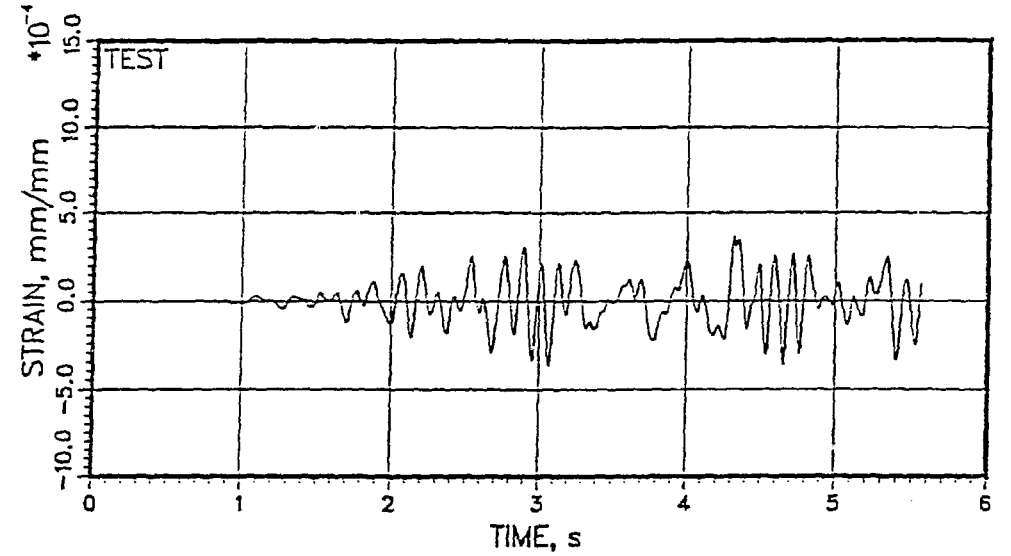

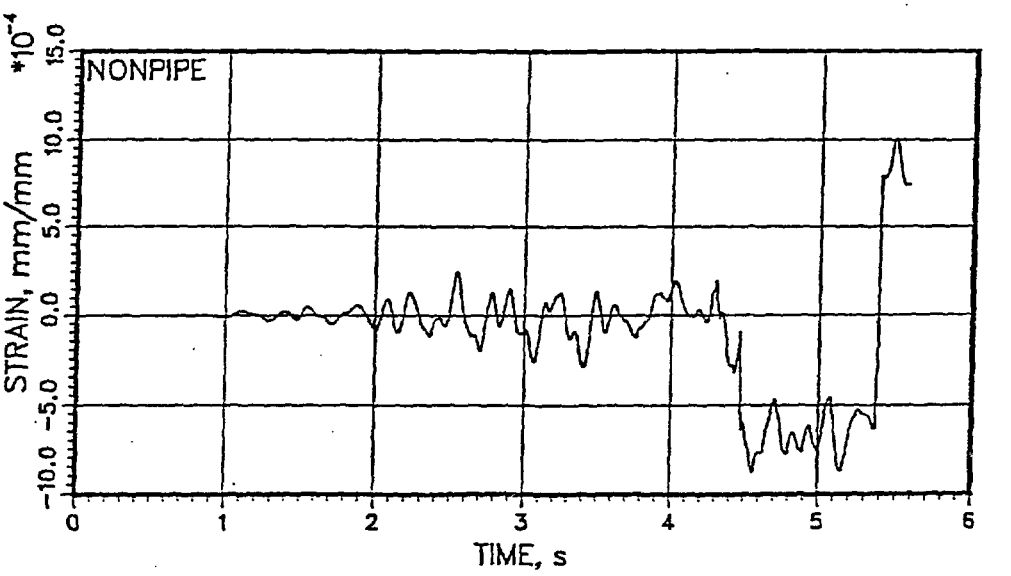

Figure 9 Comparison of measured and calculated z-bending strain at RA763

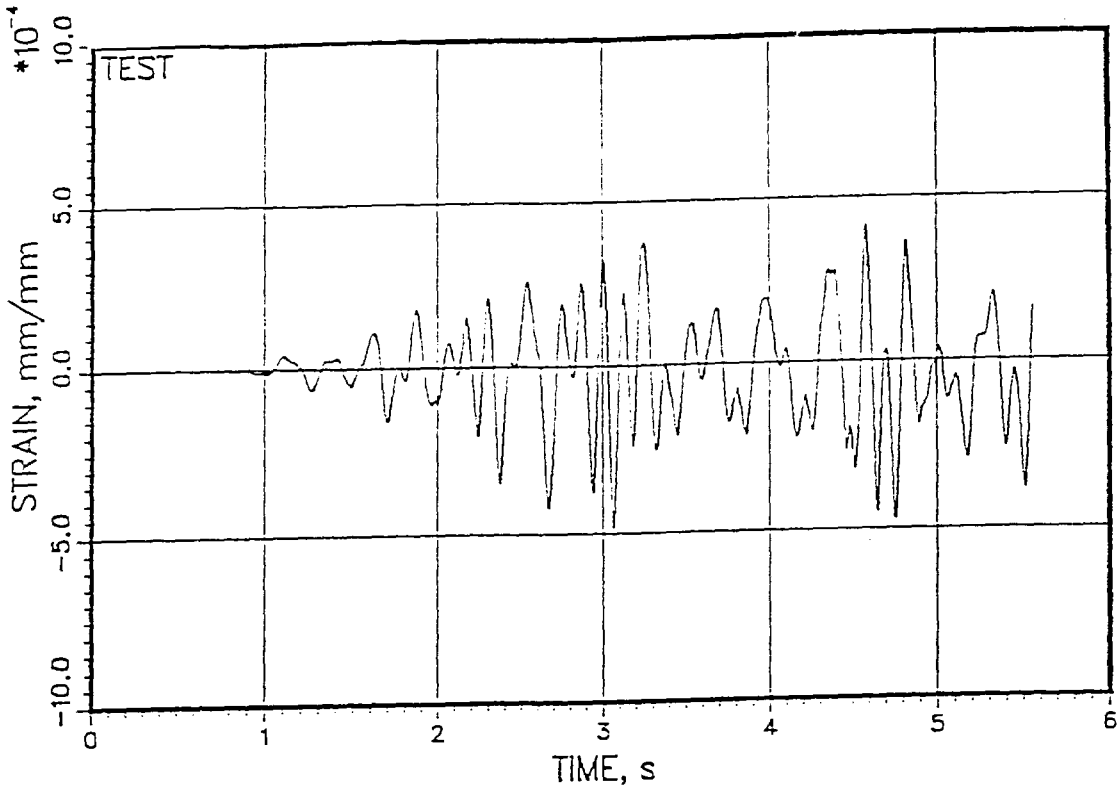

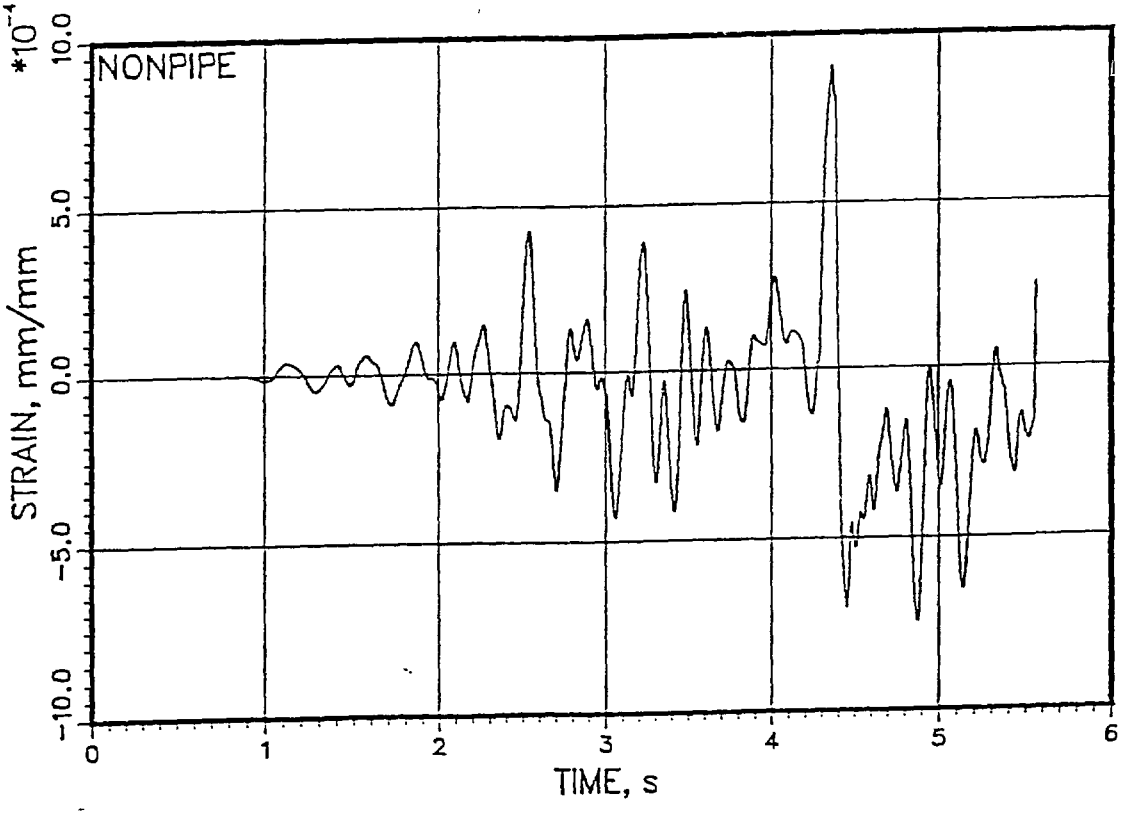

Figure 10 Comparison of measured and calculated shear strain at RA760